J|A|C|S ARTICLES

Published on Web 11/04/2009

Supramolecular Ordering in Oligothiophene−Fullerene Monolayers

Jennifer M. MacLeod,[†,||] Oleksandr Ivasenko,[‡] Chaoying Fu,[‡] Tyler Taerum,[‡] Federico Rosei,*[,†,§] and Dmitrii F. Perepichka*[,‡,§]

INRS-ÉMT, Université du Québec, 1650 Boulevard Lionel-Boulet, Varennes, Quebec, Canada J3X 1S2, and Department of Chemistry and Center for Self-Assembled Chemical Structures, McGill University, 801 Sherbrooke Street West, Montréal, Quebec, Canada H3A 2K6

Received July 31, 2009; E-mail: dmitrii.perepichka@mcgill.ca; rosei@emt.inrs.ca

Abstract: Scanning tunneling microscopy (STM) of monolayers comprising oligothiophene and fullerene molecular semiconductors reveals details of their molecular-scale phase separation and ordering with potential implications for the design of organic electronic devices, in particular future bulk heterojunction solar cells. Prochiral terthienobenzenetricarboxylic acid (TTBTA) self-assembles at the solution/graphite interface into either a porous chicken wire network linked by dimeric hydrogen bonding associations of COOH groups ($R_2^2(8)$) or a close-packed network linked in a novel hexameric hydrogen bonding motif ($R_6^6(24)$). Analysis of high-resolution STM images shows that the chicken wire phase is racemically mixed, whereas the close-packed phase is enantiomerically pure. The cavities of the chicken wire structure can efficiently host C_{60} molecules, which form ordered domains with either one, two, or three fullerenes per cavity. The observed monodisperse filling and long-range co-alignment of fullerenes is described in terms of a combination of an electrostatic effect and the commensurability between the graphite and molecular network, which leads to differentiation of otherwise identical adsorption sites in the pores.

Introduction

In recent years, significant efforts have focused on controlling the self-assembly of molecules through noncovalent directional bonding to form extended two-dimensional molecular patterns.[1−3] By carefully selecting the molecular building blocks and guiding the self-assembly process, it is possible to tailor these patterns for specific properties including geometry, chirality, and arrangement on the surface.[4,5] The ability to tune these parameters with sub-nanometer precision has led to considerable interest in engineering self-assembled molecular networks (SAMNs) for applications in molecular positioning.[6−9] Using π-functional building blocks to assemble such SAMNs offers new opportunities for molecular and thin-film organic electronics and related applications. To bridge the gap between fundamental studies of self-assembly and practical application, it is necessary to understand the behavior of molecules with properties that can be employed in technological developments.

Thiophene-containing molecules and polymers constitute a large and important class of electronic materials.[10−16] Among various materials tested for solar cells, fullerene/polythiophene composites have shown the best performance.[17−19] However, their rational optimization is rather difficult as a result of significant morphological disorder arising from both polydispersity of polythiophenes and uncontrolled (but necessary) agglomeration of fullerenes. Understanding and learning to control self-assembly in fullerene/thiophene-based systems is

† Université du Québec.
‡ Department of Chemistry, McGill University.
§ Center for Self-Assembled Chemical Structures, McGill University.
|| Current address: Dipartimento di Fisica, Università degli Studi di Trieste, Trieste, Italy

(1) De Feyter, S.; De Schryver, F. C. *Chem. Soc. Rev.* **2003**, *32*, 139.
(2) Barth, J. V. *Annu. Rev. Phys. Chem.* **2007**, *58*, 375.
(3) Barth, J. V.; Costantini, G.; Kern, K. *Nature* **2005**, *437*, 671.
(4) Barth, J. V.; Weckesser, J.; Trimarchi, G.; Vladimirova, M.; De Vita, A.; Cai, C. Z.; Brune, H.; Gunter, P.; Kern, K. *J. Am. Chem. Soc.* **2002**, *124*, 7991.
(5) Barth, J. V.; Weckesser, J.; Cai, C. Z.; Gunter, P.; Burgi, L.; Jeandupeux, O.; Kern, K. *Angew. Chem., Int. Ed.* **2000**, *39*, 1230.
(6) Theobald, J. A.; Oxtoby, N. S.; Phillips, M. A.; Champness, N. R.; Beton, P. H. *Nature* **2003**, *424*, 1029.
(7) Stepanow, S.; Lingenfelder, M.; Dmitriev, A.; Spillmann, H.; Delvigne, E.; Lin, N.; Deng, X. B.; Cai, C. Z.; Barth, J. V.; Kern, K. *Nat. Mater.* **2004**, *3*, 229.
(8) Bonifazi, D.; Kiebele, A.; Stöhr, M.; Cheng, F.; Jung, T.; Diederich, F.; Spillmann, H. *Adv. Funct. Mater.* **2007**, *17*, 1051.
(9) Cicoira, F.; Santato, C.; Rosei, F. In *STM and AFM Studies on (Bio)Molecular Systems*; Topics in Current Chemistry 285; Springer-Verlag Berlin: Berlin, 2008; pp 203−267.
(10) Mishra, A.; Ma, C. Q.; Bauerle, P. *Chem. Rev.* **2009**, *109*, 1141.
(11) *Handbook of Thiophene-Based Material: Applications in Organic Electronics and Photonics*; Perepichka, I. F., Perepichka, D. F., Eds.; John Wiley & Sons, Ltd.: New York, 2009.
(12) Perepichka, I. F.; Perepichka, D. F.; Meng, H.; Wudl, F. *Adv. Mater.* **2005**, *17*, 2281.
(13) Barbarella, G.; Melucci, M.; Sotgiu, G. *Adv. Mater.* **2005**, *17*, 1581.
(14) Fichou, D. *J. Mater. Chem.* **2000**, *10*, 571.
(15) Murphy, A. R.; Frechet, J. M. J. *Chem. Rev.* **2007**, *107*, 1066.
(16) Segura, J. L.; Martín, N.; Guldi, D. M. *Chem. Soc. Rev.* **2005**, *34*, 31.
(17) Sariciftci, N. S.; Smilowitz, L.; Heeger, A. J.; Wudl, F. *Science* **1992**, *258*, 1474.
(18) Park, S. H.; Roy, A.; Beaupre, S.; Cho, S.; Coates, N.; Moon, J. S.; Moses, D.; Leclerc, M.; Lee, K.; Heeger, A. J. *Nat. Photonics* **2009**, *3*, 297.
(19) Thompson, B. C.; Frechet, J. M. J. *Angew. Chem., Int. Ed.* **2008**, *47*, 58.

 10.1021/ja906206g CCC: $40.75

of significant importance for energy conversion applications. Several imaging techniques, including transmission electron microscopy, scanning near field optical and Raman microscopies,[19,20] and conductive atomic force microscopy,[21,22] were used to study the morphological effects in polythiophene/fullerene films, but the limited resolution and contrast of these studies has not allowed for identification of molecular species or direct observation of interactions between them. Scanning tunneling microscopy (STM) has been used for precise structural characterization of hundreds of monolayers of π-functional organic molecules and polymers,[23−28] including several multicomponent SAMNs.[8,29−35]It is thus surprising how little is known about simultaneous co-assembly of the thiophene and fullerene semiconductors. Relevant STM studies were reported for fullerene co-assembly with two cyclic oligothiophenes, which can hardly be synthesized in amounts sufficient for large-scale materials applications.[30,36a] Most recently, a more synthetically accessible star-shaped oligothiophene was reported to co-assembly with fullerene in a SAMNs controlled by weak van der Walls interactions.[36b]

In this work we describe the use of H-bonding to control the self-organization of oligothiophene semiconductors. Using STM, we demonstrate formation of highly ordered 2D networks of the COOH-substituted oligothiphene TTBTA and highlight an unusual H-bonding motif. We discuss manifestations of chirality and demonstrate that thiophene−fullerene interactions, as well as fullerene−fullerene interactions, lead to monodispersed C_{60} confinement and long-range co-alignment within a porous network.

Results and Discussion

Design of the Model System. Trimesic acid (TMA) has been widely used to study various aspects of self-assembly via H-bonding in both 2D[37−39] and 3D.[40,41] Several TMA homologues (Supporting Information) with a larger molecular size

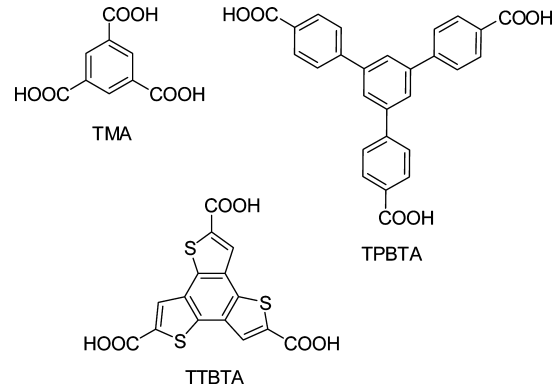

have been studied, e.g., triphenylbenzenetricarboxylic acid (TPBTA)[42−44] and some others,[45,46] and their behavior is also well understood. The aromatic core of these molecules facilitates their adsorption on surfaces and defines the periodicity of the formed H-bonded lattice but usually has no other function. On the other hand, designing π-functional molecules (e.g., with semiconducting or light-emitting properties) with directional interactions suitable for self-assembly could lead to important practical applications. Because of the increasing technological importance of π-conjugated thiophene derivatives, we have decided to study their self-assembly on surfaces. Choosing an oligothiophene that mimics the TMA structure makes its self-assembly more predictable and easier to control. The simple replacement of TMA's benzene core with a thiophene is not acceptable because of the low symmetry of the latter. We instead chose to study the C_{3h}-symmetric molecule terthienobenzenetricarboxylic acid (TTBTA), a π-functional member of the class of C_3-symmetric carboxylic acids including TMA and TPBTA. We note that other star-shaped derivatives of terthienobenzene have attracted interest as semiconductors for photovoltaic applications[47] and as building blocks for conducting polymers with suppressed polaron recombination.[48]

Unlike TMA and TPBTA, TTBTA is prochiral. Specifically, switching between *R* and *S* enantiomers (Figure 1) results in a 57° rotation of the triangle defined by thiophene sulfur atoms, well above the typical errors of STM measurements (<5°). Assuming that submolecular features in the TTBTA can be related to the sulfur atom (see below), the enantiomers should thus be easily distinguishable.

(20) Gao, Y.; Grey, J. K. *J. Am. Chem. Soc.* **2009**, *131*, 9654.
(21) Pingree, L. S. C.; Reid, O. G.; Ginger, D. S. *Nano Lett.* **2009**, *9*, 2946.
(22) Bull, T. A.; Pingree, L. S. C.; Jenekhe, S. A.; Ginger, D. S.; Luscombe, C. K. *ACS Nano* **2009**, *3*, 627.
(23) Ahmed, M. O.; Wang, C. M.; Keg, P.; Pisula, W.; Lam, Y. M.; Ong, B. S.; Ng, S. C.; Chen, Z. K.; Mhaisalkar, S. G. *J. Mater. Chem.* **2009**, *19*, 3449.
(24) Zhang, J.; Li, B.; Cui, X.; Wang, B.; Yang, J.; Hou, J. G. *J. Am. Chem. Soc.* **2009**, *131*, 5885.
(25) Sakaguchi, H.; Matsumura, H.; Gong, H.; Abouelwafa, A. M. *Science* **2005**, *310*, 1002.
(26) Lafferentz, L. *Science* **2009**, *321*, 1193.
(27) Plass, K. E.; Grzesiak, A. L.; Matzger, A. J. *Acc. Chem. Res.* **2007**, *40*, 287.
(28) Furukawa, S.; De Feyter, S. In *Topics in Current Chemistry, Vol. 287 (Templates in Chemistry III)*; Springer-Verlag: Berlin, 2009; pp 87−133.
(29) Scudiero, L.; Hipps, K. W.; Barlow, D. E. *J. Phys. Chem. B* **2003**, *107*, 2903.
(30) Mena-Osteritz, E.; Bäuerle, P. *Adv. Mater.* **2006**, *18*, 447.
(31) Ivasenko, O.; MacLeod, J. M.; Chernichenko, K. Y.; Balenkova, E. S.; Shpanchenko, R. V.; Nenajdenko, V. G.; Rosei, F.; Perepichka, D. F. *Chem. Commun.* **2009**, *10*, 1192.
(32) Barlow, D. E.; Scudiero, L.; Hipps, K. W. *Langmuir* **2004**, *20*, 4413.
(33) Madueno, R.; Raisanen, M. T.; Silien, C.; Buck, M. *Nature* **2008**, *454*, 618.
(34) Jin, W.; Dougherty, D. B.; Cullen, W. G.; Robey, S.; Reutt-Robey, J. E. *Langmuir* **2009**, *25*, 9857.
(35) Ma, X. J.; Li, Y. B.; Qiu, X. H.; Zhao, K. Q.; Yang, Y. L.; Wang, C. *J. Mater. Chem.* **2009**, *19*, 1490.
(36) (a) Pan, G. B.; Cheng, X. H.; Hoger, S.; Freyland, W. *J. Am. Chem. Soc.* **2006**, *128*, 4218. (b) Piot, L.; Silly, F.; Tortech, L.; Nicolas, Y.; Blanchard, P.; Roncali, J.; Fichou, D. *J. Am. Chem. Soc.* **2009**, *131*, 12864.
(37) Kudernac, T.; Lei, S. B.; Elemans, J.; De Feyter, S. *Chem. Soc. Rev.* **2009**, *38*, 402.
(38) Nath, K. G.; Ivasenko, O.; MacLeod, J. M.; Miwa, J. A.; Wuest, J. D.; Nanci, A.; Perepichka, D. F.; Rosei, F. *J. Phys. Chem. C* **2007**, *111*, 16996.
(39) Nath, K. G.; Ivasenko, O.; Miwa, J. A.; Dang, H.; Wuest, J. D.; Nanci, A.; Perepichka, D. F.; Rosei, F. *J. Am. Chem. Soc.* **2006**, *128*, 4212.
(40) Zaworotko, M. J. *Chem. Commun.* **2001**, 1.
(41) Kolotuchin, S. V.; Thiessen, P. A.; Fenlon, E. E.; Wilson, S. R.; Loweth, C. J.; Zimmerman, S. C. *Chem.−Eur. J.* **1999**, *5*, 2537.
(42) Kampschulte, L.; Lackinger, M.; Maier, A. K.; Kishore, R. S. K.; Griessl, S.; Schmittel, M.; Heckl, W. M. *J. Phys. Chem. B* **2006**, *110*, 10829.
(43) Kampschulte, L.; Werblowsky, T. L.; Kishore, R. S. K.; Schmittel, M.; Heckl, W. M.; Lackinger, M. *J. Am. Chem. Soc.* **2008**, *130*, 8502.
(44) Ruben, M.; Payer, D.; Landa, A.; Comisso, A.; Gattinoni, C.; Lin, N.; Collin, J.-P.; Sauvage, J.-P.; De Vita, A.; Kern, K. *J. Am. Chem. Soc.* **2006**, *128*, 15644.
(45) Xiao, W.; Feng, X.; Ruffieux, P.; Gröning, O.; Müllen, K.; Fasel, R. *J. Am. Chem. Soc.* **2008**, *130*, 8910.
(46) Gutzler, R.; Lappe, S.; Mahata, K.; Schmittel, M.; Heckl, W. M.; Lackinger, M. *Chem. Commun.* **2009**, 680.
(47) de Bettignies, R.; Nicolas, Y.; Blanchard, P.; Levillain, E.; Nunzi, J. M.; Roncali, J. *Adv. Mater.* **2003**, *15*, 1939.
(48) Taerum, T.; Lukoyanova, O.; Wylie, R. G.; Perepichka, D. F. *Org. Lett.* **2009**, *11*, 3230.

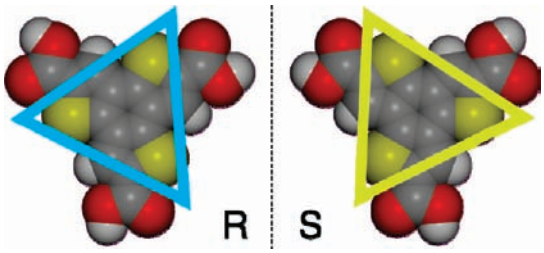

Figure 1. Relationship between *R* and *S* enantiomers of TTBTA. The rotation between the triangles defined by the sulfur atoms is 57°.

Finally, we investigated the effect of a perturbation to the building block on the host−guest chemistry. As the guest we chose fullerene (C_{60}) both because of its technological importance as n-type semiconductor for photovoltaic cells, particularly in heterojunctions with oligo-/polythiophenes,[49−51] and because its behavior as a guest molecule in 2D inclusion networks is well understood.[30,52−57]

TTBTA Polymorphism. Supramolecular architecture is defined by the geometry of the building blocks and the linking mode of their functional groups. Carboxylic functional groups are known to self-associate[58] through either cyclic dimers (Figure 2a), cyclic trimers (Figure 2b), cyclic tetramers (Figure 2c),[59] as well as linear dimers (Figure 2d)[42] and chains (Figure 2e). In TMA, combinations of the first two produce a family of hexagonal motifs (polymorphs) extending from the fully dimeric "chicken wire" structure to the fully trimeric "super-flower" structure.[60−62] By tuning the size and the shape of a building block, along with the number and orientation of carboxylic groups, a variety of 2D SAMNs have been prepared. Like a large number of these other molecules, TTBTA self-assembles readily through a dimeric hydrogen bonding and forms a hexagonal open-pored chicken wire network (Figure 3). Its periodicity (2.45 ± 0.16 nm) and the diameter of the pores (∼1.84 nm) are dictated by the geometry of the terthienobenzene core and are larger than those of the TMA chickenwire network (1.6 nm and ∼1.1 nm, respectively[55]). Similar to the TMA chicken wire network,[60] we occasionally observe brighter contrast indicative of a "guest" TTBTA molecule trapped metastably within a cavity (see Supporting Information).

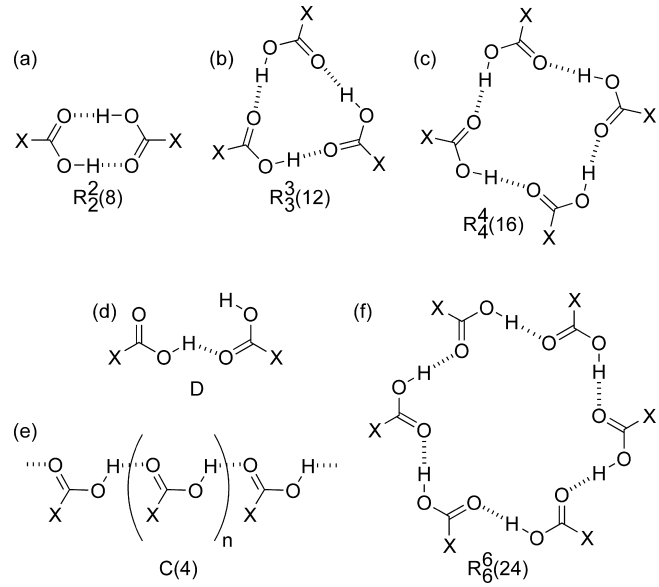

Figure 2. Most common modes of carboxylic self-association: (a) cyclic dimer, (b) cyclic trimer, (c) cyclic tetramer, (d) linear dimer, and (e) chain. Panel f shows a cyclic hexamer. The graph-set nomenclature[63] for each association is provided beneath the schematic.

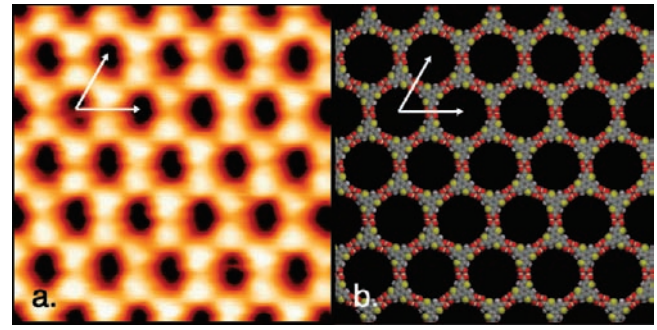

Figure 3. STM image (a) and model (b) of the TTBTA chicken wire structure, formed at the HOPG/heptanoic acid interface. Lattice vectors are indicated in white. The experimental (calculated) lattice vector lengths are 2.45 ± 0.16 nm (2.39 nm) separated by an angle of 60°. STM image parameters: $V_b = -800$ mV, $I_t = 0.2$ nA, area 12.9 nm × 12.9 nm.

In contrast to TMA, we did not observe domains of flower structure. However, a completely new polymorph, based on hexameric association of the molecules (Figure 4), was observed at high solution concentrations. This densely packed structure has a hexagonal unit cell, with a lattice vector of 1.82 ± 0.13 nm. Henceforth, we refer to it as the close-packed phase.

Density functional theory (DFT) calculations at B3LYP/6-31G(d,p) level were performed to identify the bonding motif of the close-packed phase (Figure 4b). Among several possible hexameric association modes of TTBTA, the cyclic hydrogen-bonded hexamer of carboxylic groups, $R_6^6(24)$ (Figure 2f), was found to be the most stable.

We note that such cyclic hexameric hydrogen bonding of carboxylic groups has not been observed before in 2D structures.[64] To understand what governs the formation of this

(49) Padinger, F.; Rittberger, R. S.; Sariciftci, N. S. *Adv. Funct. Mater.* **2003**, *13*, 85.
(50) Li, G.; Shrotriya, V.; Huang, J. S.; Yao, Y.; Moriarty, T.; Emery, K.; Yang, Y. *Nat. Mater.* **2005**, *4*, 864.
(51) Kim, Y.; Cook, S.; Tuladhar, S. M.; Choulis, S. A.; Nelson, J.; Durrant, J. R.; Bradley, D. D. C.; Giles, M.; McCulloch, I.; Ha, C. S.; Ree, M. *Nat. Mater.* **2006**, *5*, 197.
(52) Meier, C.; Landfester, K.; Ziener, U. *J. Phys. Chem. C* **2008**, *112*, 15236.
(53) Stöhr, M.; Wahl, M.; Spillmann, H.; Gade, L. H.; Jung, T. A. *Small* **2007**, *3*, 1336.
(54) Li, M.; Deng, K.; Lei, S. B.; Yang, Y. L.; Wang, T. S.; Shen, Y. T.; Wang, C. R.; Zeng, Q. D.; Wang, C. *Angew. Chem., Int. Ed.* **2008**, *47*, 6717.
(55) Griessl, S. J. H.; Lackinger, M.; Jamitzky, F.; Markert, T.; Hietschold, M.; Heckl, W. M. *J. Phys. Chem. B* **2004**, *108*, 11556.
(56) Kiebele, A.; Bonifazi, D.; Cheng, F. Y.; Stöhr, M.; Diederich, F.; Jung, T.; Spillmann, H. *ChemPhysChem* **2006**, *7*, 1462.
(57) Spillmann, H.; Kiebele, A.; Stohr, M.; Jung, T. A.; Bonifazi, D.; Cheng, F. Y.; Diederich, F. *Adv. Mater.* **2006**, *18*, 275.
(58) Lackinger, M.; Heckl, W. M. *Langmuir* **2009**, *25*, 11307.
(59) Eichhorst-Gerner, K.; Stabel, A.; Moessner, G.; Declerq, D.; Valiyaveettil, S.; Enkelmann, V.; Müllen, K.; Rabe, J. P. *Angew. Chem., Int. Ed. Engl.* **1996**, *35*, 1492.
(60) Griessl, S.; Lackinger, M.; Edelwirth, M.; Hietschold, M.; Heckl, W. M. *Single Mol.* **2002**, *3*, 25.
(61) Ye, Y. C.; Sun, W.; Wang, Y. F.; Shao, X.; Xu, X. G.; Cheng, F.; Li, J. L.; Wu, K. *J. Phys. Chem. C* **2007**, *111*, 10138.
(62) MacLeod, J. M.; Ivasenko, O.; Perepichka, D. F.; Rosei, F. *Nanotechnology* **2007**, *18*, 424031.
(63) Grell, J.; Bernstein, J.; Tinhofer, G. *Acta Crystallogr.* **1999**, *B55*, 1030.

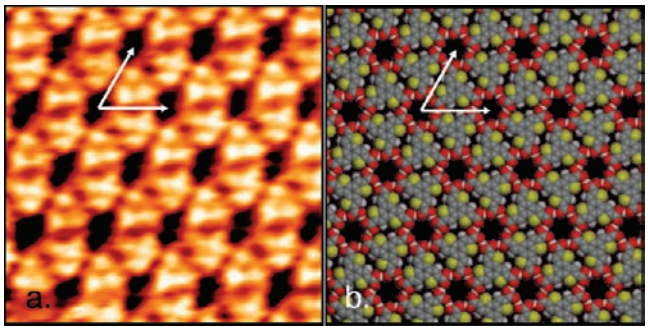

Figure 4. STM image (a) and model (b) of the TTBTA close-packed structure, formed at the HOPG/heptanoic acid interface. Lattice vectors are indicated in white. The experimental (calculated) lattice vector lengths are 1.82 ± 0.13 nm (1.66 nm) separated by an angle of 60°. STM image parameters: $V_b = -400$ mV, $I_t = 0.1$ nA, area 7.5 nm × 7.5 nm.

Table 1. Stabilization Energies (B3LYP 6-31G(d,p)) and Relative Packing Efficiencies of Different Hydrogen-Bonding Motifs for Selected Carboxylic Acids

	energy (kcal/mol)[a]			
association type	FA	BA	TMA	TTBTA
$R_2^2(8)$	9.82	10.19	10.01	10.20
$R_3^3(12)$	8.79	8.74	8.78	8.92
$R_6^6(24)$	10.09	7.96	7.53	8.94

[a] Per carboxylic group that participates in the H-bonding.

unusual polymorph, we performed series of DFT calculations (Table 1) for different associates of TTBTA, TMA, TPBTA, benzoic (BA) and formic acid (FA). All calculations were performed in vacuo, which appears to provide a reasonable approximation for the solution phase, e.g. the calculated stabilization energy of $R_2^2(8)$ dimers is close to the value of association enthalpy (∼9 kcal/mol) measured in nonpolar solvents.[65]

As is evident from Table 1, of the three possible association types, the stabilization energies for the carboxylic hexamers are the most sensitive to changes in molecular structure. This can be rationalized in view of secondary interactions between neighboring molecules due to their close proximity (approaching van der Waals distances). Specifically, TMA hexamers are energetically disfavored with respect to TMA trimers due to excessive steric repulsion between the aromatic cores.

The relative stability of the SAMN polymorphs is defined by the previously discussed intermolecular interactions as well as molecule−substrate interactions. To account for the latter, we compare the packing efficiencies of the different polymorphs (Table 2), assuming that in the first approximation the strength of these weak molecule−surface interactions is proportional to the molecular density (coverage). The close-packed polymorph exhibits the highest packing efficiency, and unlike the other three polymorphs, its relative packing efficiency depends strongly on the size of the building block. The larger molecules can thus pack more efficiently in the close-packed polymorph, leading to stronger SAMN/substrate interactions.

SAMN−substrate interactions also account for observed rotation between the SAMN lattice and the underlying HOPG. Commensurability of the chicken wire lattice is obtained when

Table 2. Relative Packing Efficiencies of Several Polymorphs of Tricarboxylic Acid Based SAMNs

		packing efficiency[a]		
polymorph	H-bonding motif	TMA	TTBTA	TPBTA
chicken wire	$R_2^2(8)$	**1**	**1**	**1**
flower	$R_2^2(8) + R_3^3(12)$	**1.24**	1.31	1.30
superflower	$R_3^3(12)$	**1.60**[b]	1.74	1.78
close packed	$R_6^6(24)$	1.78	**2.21**	2.65

[a] Calculated as the ratio of the molecular surface density of a given polymorph to the molecular surface density of the corresponding chicken wire polymorph with the numbers in bold reflecting that this polymorph was experimentally observed (the molecular structures of the flower and superflower structures are given in the Supporting Information). [b] This polymorph was only observed in ultrahigh vacuum.[61]

the TMA, TTBTA and TPBTA lattices are rotated by 5°,[66] 21° (Supporting Information), and 22°,[58] respectively, from the HOPG lattice. This structural detail has implications not only for the formation of superlattices in 2D[67] but also for the behavior of guest molecules, for example, in the TMA/coronene system[66] (see also host−guest interactions below).

Chirality. 2D confinement at a surface provides a convenient testing ground to discern the relationship between structure and chirality at the nano scale.[45,68,69] Among the current challenges in this area, identification of the minimum requirements to induce enantiomorphism on surfaces is of fundamental interest.[70]

TTBTA is a prochiral molecule, and its chiral signature in 2D confined space can be revealed in high-resolution STM images. The submolecular structure of TTBTA manifests as three bright dots defining an equilateral triangle. The observed position of and distance between the dots (5.4 ± 1.0 Å) matches the calculated S···S distance in TTBTA (5.40 Å), and they were therefore used to identify the enantiomeric composition of TTBTA polymorphs. This was done by fitting an equilateral triangle to the three-dot pattern of each molecule.[71]

The histogram of rotation angles for the chicken wire polymorph (Figure 5b) exhibits a clear bimodal distribution with two maxima separated by ∼55°, in agreement with the predicted difference between *R* and *S* TTBTA enantiomers. A detailed analysis reveals approximately equal numbers of randomly intermixed *R* and *S* enantiomers, which allows us to characterize the TTBTA chicken wire polymorph as a highly ordered racemic SAMN. Conversely, analysis of images of the close-packed phase with submolecular resolution shows no evidence for racemic intermixing (Figure 5d); every domain is an enantiomerically pure conglomerate.

The different behavior of the two polymorphs with respect to chirality is elucidated through ab initio (HF/3-21G**) calculations of the diastereomeric hexamers of these TTBTA polymorphs, which are presented in the Table 3.

(64) However, a similar $R_6^6(24)$ assembly was recently observed in a 3D crystal: Maspoch, D.; Domingo, N.; Roques, N.; Wurst, K.; Tejada, K.; Rovira, C.; Ruiz-Molina, D.; Veciana, J. *Chem.−Eur. J.* **2007**, *13*, 8153.
(65) Kolbe, A.; Demus, D. *Z. Naturforsch.* **1968**, *A 23*, 1237.
(66) Griessl, S. J. H.; Lackinger, M.; Jamitzky, F.; Markert, T.; Hietschold, M.; Heckl, W. A. *Langmuir* **2004**, *20*, 9403.
(67) Li, M.; Deng, K.; Yang, Y.-L.; Zeng, Q.-D.; He, M.; Wang, C. *Phys. Rev. B* **2007**, *76*, 155438.
(68) Fasel, R.; Parschau, M.; Ernst, K. H. *Nature* **2006**, *439*, 449.
(69) Lorenzo, M. O.; Baddeley, C. J.; Muryn, C.; Raval, R. *Nature* **2000**, *404*, 376.
(70) Elemans, J. A. A. W.; De Cat, I.; Xu, H.; De Feyter, S. *Chem. Soc. Rev.* **2009**, *38*, 722.
(71) Although the three-dot patterns match the S···S distance, we do not unequivocally assign the bright contrast to the S atoms. It is likely that the contrast originates near, but not necessarily on, the S atoms. We have fitted triangles to the S atoms in Figure 5a and c in order to clarify our definition of the enantiomers in the corresponding STM images.

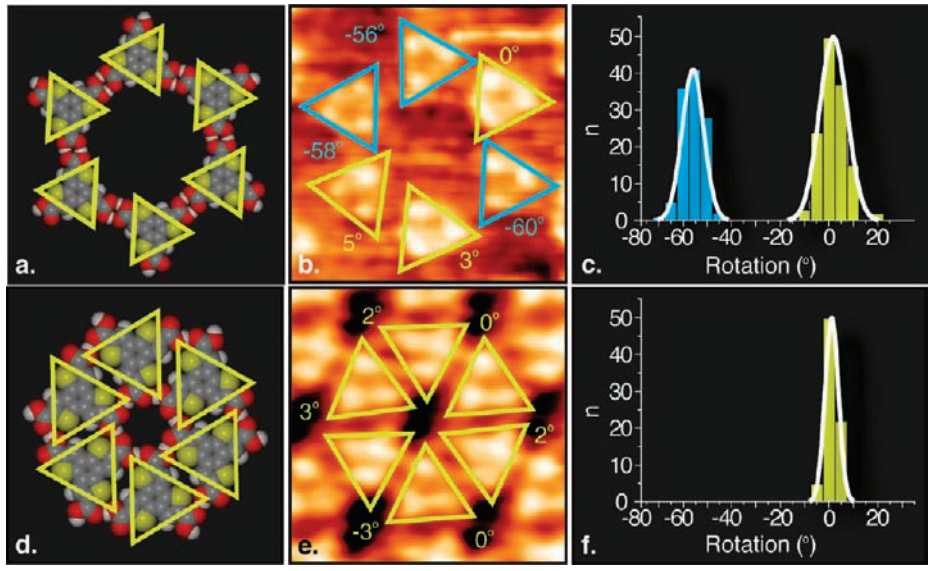

Figure 5. Enantiomeric composition of chicken wire (a−c) and close-packed (d−f) phases of TTBTA. The STM images (b and e) demonstrate the measurement of molecular rotation within a hexamer of each structure; the histograms (c and f) show the distribution of rotational angles over an entire domain. STM image parameters: $V_b = -1000$ mV, $I_t = 0.3$ nA, area 4.6 nm × 4.6 nm (b); $V_b = -400$ mV, $I_t = 0.1$ nA, area 3.8 nm × 3.8 nm (e).

Table 3. Relative Destabilization Energies of Diastereomeric Cyclic Hexamers of TTBTA

	relative energy, kcal/mol	
diastereomer	chicken wire polymorph	close-packed polymorph
R,R,R,R,R,R	0	0
R,R,R,R,R,S	0.77	7.1
R,R,R,R,S,S	1.56	13.7
R,R,R,S,R,S	1.51	13.8
R,R,S,R,R,S	1.52	13.4
R,R,R,S,S,S	2.31	19.8
R,R,S,R,S,S	2.28	19.9
R,S,R,S,R,S	2.22	20.1

These findings echo our assessment of the stability of different polymorphs for various building blocks. Once again the close proximity of the molecular cores in the close-packed phase results in van der Waals repulsion that significantly destabilizes H-bonding in racemic mixtures when compared to H-bonding in enantiomerically pure conglomerates. Conversely, the chicken wire hexamers do not meet the energy baseline for enantiomeric induction. There are no interactions between the TTB cores, and thus the racemic solid solution is formed.

TTBTA-C_{60} Host−Guest Architectures. In host−guest systems formed at the solution/solid interface, fullerenes have been shown to adsorb predominantly within the host cavities,[54,55,62] although adsorption on top of the host molecules has been reported for oligothiophene macrocycles, which are topologically predisposed to form π-complexes with fullerenes.[30,36] The hexagonal cavity of the TMA SAMN hosts a single fullerene molecule.[55] On the basis of the estimated pore size of the TTBTA chicken wire, up to three fullerene molecules can be accommodated in each cavity.

Adding fullerene to the TTBTA solution on HOPG results in the formation of TTBTA−fullerene host−guest structures. The fullerene molecules appear as bright, round protrusions with no submolecular resolution in the STM images and can therefore be distinguished from the TTBTA molecules. Figure 6 shows images where it is possible to identify fullerene monomers, dimers, and trimers, respectively. Remarkably, the fullerenes exhibit strong co-alignment and monodispersed filling, forming into domains with equivalent fullerene count and positioning within each TTBTA chicken wire cavity. For TTBTA × $1C_{60}$ domains, the fullerenes are positioned asymmetrically in the cavity (cf. Supporting Information). This ordering of C_{60} usually extends to a complete domain of the TTBTA host network. At the interface of two TTBTA domains of network circularly ordered structures of C_{60} have been occasionally observed (see Supporting Information). Although we did not systematically vary the concentration of C_{60} in order to investigate the concentration−filling relationship,[72] we note that domains with different fullerene occupancies (TTBTA × $1C_{60}$ and TTBTA × $2C_{60}$) were observed to coexist on the same surface.

The bright appearance of the fullerene molecules makes it difficult to directly identify their bonding site (i.e., on-top or in-cavity) for completely filled monolayers, since the TTBTA lattice cannot be easily discerned. However, the in-cavity adsorption is evident at low coverage, where both filled and empty parts of TTBTA networks can be clearly identified (Figure 6a). Furthermore, no fullerene adsorption was observed on the close-packed polymorph, which lacks cavities, indicating that on-top adsorption is not favorable (cf. Supporting Information). This is not surprising since the in-cavity position allows fullerene molecules to interact favorably with both the HOPG surface below and with a TTBTA molecule beside it, most likely through $C_{60}\cdots S$ contacts.[73] We also note that fullerene adsorption is much less efficient in the SAMN of TMA, which lacks $C_{60}\cdots S$ interactions; only partial filling (to a maximum of approximately 1 fullerene per 4 cavities) could be achieved in the TMA network under these conditions.[55,62]

Considering only the geometry of the TTBTA chicken wire structure, the hexameric cavity could be expected to provide six equivalent sites for C_{60} adsorption. However, this simplified scenario does not explain the reason for the striking co-alignment of C_{60} within SAMN domains (Figure 6). To account for such long-range ordering, one has to assume either that the six

(72) Meier, C.; Landfester, K.; Kunzel, D.; Markert, T.; Gross, A.; Ziener, U. *Angew. Chem., Int. Ed.* **2008**, *47*, 3821.
(73) Fomina, L.; Reyes, A.; Fomine, S. *Int. J. Quantum Chem.* **2002**, *89*, 477.

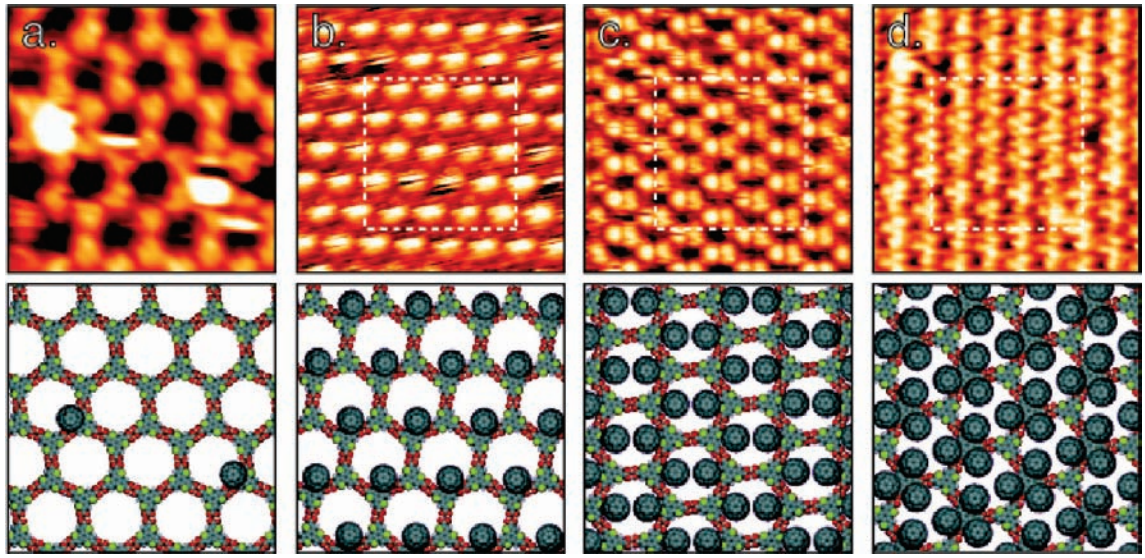

Figure 6. TTBTA-C_{60} host−guest architectures with sparse fullerene coverage (a) and one (b), two (c), and three (d) fullerenes per chicken wire unit cell. Tentative molecular models have been assigned to a 10.7 nm × 10.7 nm area of each image (indicated by dashed boxes in b−d). STM image parameters: $V_b = -1000$ mV, $I_t = 0.1$ nA (a); $V_b = -600$ mV, $I_t = 0.1$ nA (b); $V_b = -900$ mV, $I_t = 0.03$ nA (c); $V_b = -800$ mV, $I_t = 0.3$ nA (d). Image a has an area of 10.7 nm × 10.7 nm; images b−d each have an area of 18 nm × 18 nm.

adsorption sites in the TTBTA hexamer are not equivalent or that long-range electronic interactions take place between fullerenes.[74] Our analysis below suggests that both mechanisms are plausible and that both are likely to contribute synergistically to the observed co-alignment.

Fullerene is an electron-acceptor molecule that can participate in charge transfer interactions with both oligothiophene TTBTA and with HOPG. As a result of this interaction, C_{60} molecules acquire partial negative charge and will experience long-range ($E \sim 1/r$) electrostatic repulsion above the plane of the TTBTA network. To minimize this repulsion, the system will maximize the $C_{60}\cdots C_{60}$ spacing while maintaining favorable $C_{60}\cdots$TTBTA and $C_{60}\cdots$HOPG interactions, leading to the observed well-ordered patterns. The same effect can also explain the monodispersed filling of the host network: adding a second (third) molecule to an already populated cavity will reduce the spacing between the fullerenes of adjacent cavities, leading to larger Coulombic repulsion.

However, even when the degree of charge transfer is assumed at 33% (i.e., 1/3 e per C_{60}), the difference between the Coulombic repulsion energies of the ordered and disordered states should not exceed ~0.33 kcal/mol for the TTBTA × 1C_{60} SAMN (see Supporting Information). This is lower than the thermal energy at room temperature ($RT = 0.6$ kcal/mol) and is unlikely to be the sole mechanism for the co-alignment. We note, however, that higher order electrostatic interactions (such as dipole−dipole interactions) could also contribute to the observed ordering phenomenon.[75] In fact, similar spontaneous ordering of fullerenes has been observed in a host−guest network of oligothiophene macrocycles populated with C_{60}.[30] In this case, the ordering was attributed exclusively to electrostatic effects (quadrupole interactions) introduced by the charge transfer associated with fullerene−thiophene complexation.

In the TTBTA/C_{60} system, the mutual substrate/SAMN orientation is also very likely to play a role in the fullerene positioning. The rotation of the TTBTA lattice with respect to the underlying HOPG lattice breaks the degeneracy of the six equivalent lattice sites for C_{60} within the cavity (see Supporting Information). Occupation of a single site within each pore should be favored, since only one site will have the optimal combination of $C_{60}\cdots$TTBTA and $C_{60}\cdots$HOPG interactions. This site would thus be the first one occupied, and successive fullerenes will go into the second most favorable site. Since the TTBTA$\cdots C_{60}$ interactions in all six sites are equivalent, their inequivalency can be fully attributed to different HOPG$\cdots C_{60}$ interactions. Thus, the corrugation of the potential energy for C_{60} adsorbed on HOPG (0.30 kcal/mol[76]) could be a good approximation for the ordering energy. This is still lower than *RT*, which is confirmed by the fact that at incomplete filling (one C_{60} per several cavities), when electrostatic ordering is not at work, the fullerene diffuses freely inside the cavity and appears as a larger protrusion in the STM image (Figure 6a).

On the other hand, this HOPG-induced ordering can and should act simultaneously and synergistically with electrostatic ordering. The sum of the two could thus be expected to overcome the thermal disorder at room temperature.

Conclusions

In summary, we have described the self-assembly of the prochiral oligothiophene building block TTBTA at the solution−solid interface. Long-range ordering is mediated by hydrogen-bonding of its carboxylic groups. In addition to the porous chicken wire polymorph comprising the expected dimeric bonding motif, we identified a close-packed phase based on a new hexameric ($R_6^6(24)$) hydrogen-bonded macrocycle. The enantiomorphism in the polymorphs of prochiral TTBTA is controlled by intermolecular interactions: whereas the chicken wire polymorph is racemically disordered, the increased interaction in the close-packed phase leads to a racemically pure

(74) The closest spacing between fullerenes of adjacent cavities (0.12 nm) is larger than the double van der Waals radius of C_{60} (0.09 nm), and thus ordering due to short-range interactions is improbable.

(75) Although such interactions are quite difficult to estimate quantitatively, we expect them to be somewhat less important because of the relatively shorter range of dipole−dipole electrostatic forces ($E \sim 1/r^3$).

(76) Gravil, P. A.; Devel, M.; Lambin, P.; Bouju, X.; Girard, C.; Lucas, A. A. *Phys. Rev. B* **1996**, *53*, 1622.

structure. Introducing fullerenes to the solution demonstrated that the chicken wire structure can host one, two, or three C_{60} guests per pore. The specific fullerene−thiophene interactions appear to significantly increase the efficiency of fullerene adsorption as compared with similar SAMN of trimesic acid on HOPG, which lacks such interactions. The resulting charge transfer acts synergistically with the symmetry breaking introduced by the relative orientation of the TTBTA lattice with respect to the underlying HOPG, allowing for precise spatial localization (long-range ordering) over various fullerene stoichiometries. We speculate that using such ordered monolayers as templates for growing multilayer materials (as, e.g., in ref 31) could lead to a molecularly defined bulk heterojunction film leading to significantly improved efficiency of organic photovoltaic devices.

Experimental Section

The synthesis of TTBTA is described in detail elsewhere.[48]

Graphite (grade SPI-2) was obtained from SPI Supplies and was cleaved prior to each experiment using adhesive tape. Heptanoic (99%) and octanoic acid (98%) were purchased from Sigma-Aldrich and were used without further purification. Molecular networks formed immediately upon deposition of the saturated TTBTA solution on the HOPG surface. Octanoic and heptanoic acids, as well as octanol, can all be used to prepare TTBTA networks, whereas no self-assembly was observed in less polar solvents such as trichlorobenzene, presumably due to very low solubility of TTBTA. In the host−guest experiments a small amount of fullerene (~0.5 mg) was suspended in few drops of saturated TTBTA solution prior to deposition onto the HOPG or a saturated C_{60} solution was applied to a pre-existing TTBTA network.

STM images were acquired using either a NanoSurf EasyScan 2 or a Digital Instruments Inc. (Veeco) NanoScope IIIa. Both microscopes were operated at ambient conditions, and data were obtained from the topography channel. Tips were cut from 80/20 Pt/Ir wire. Calibration of the piezoelectric positioners was verified by atomic resolution imaging of graphite (*x*- and *y*-directions) and by the height of single steps on the graphite surface (*z*-direction). Atomic resolution was verified prior to the addition of molecular solutions to the surface. Image processing was performed with the WSxM software.[77] The periodicity of the chicken wire lattice was determined from images where the underlying HOPG lattice was imaged in the same frame. The periodicity of the close-packed structure was determined from images where the chicken wire lattice was imaged in the same frame; the uncertainty on the chicken wire lattice measurement was propagated to the close-packed measurements.

Ab initio calculations of diastereomeric hexamers for TTBTA chicken wire and close-packed phases were performed in Gaussian 03W.[78] All DFT calculations were performed with PC GAMESS-(Firefly).[79] In both cases default convergence criteria and the highest possible symmetry restrictions were used.

Acknowledgment. We thank Dr. J. Lipton-Duffin for a critical reading of the manuscript. This work was supported by the NSERC of Canada and the FQRNT (Quebec). D.F.P. acknowledges the DuPont Young Professor Award. F.R. acknowledges partial salary support from the Canada Research Chairs program. C.F. acknowledges CSACS summer research award.

Supporting Information Available: Molecular structures for TMA homologues for which SAMNs have been studied; molecular structures and areal densities of all TTBTA polymorphs; structure of a (hypothetical) TMA hexamer including H···H distances; domain orientation of both SAMNs; STM image showing coexisting domains of close-packed and chicken wire in the presence of fullerenes; image showing TTBTA guest in TTBTA chicken wire cavity; complete ref 78; additional details (figures/geometries/energies) for *ab initio* calculations of diastereomeric hexamers. This material is available free of charge via the Internet at http://pubs.acs.org.

JA906206G

(77) Horcas, I.; Fernandez, R.; Gomez-Rodriguez, J. M.; Colchero, J.; Gomez-Herrero, J.; Baro, A. M. *Rev. Sci. Instrum.* **2007**, *78*, 013705.
(78) Frisch, M. J. et al. *Gaussian 03, Revision D.01*; Gaussian, Inc.: Wallingford, CT, 2004.
(79) Granovsky, A. A. PC Gamess/Firefly, 7.1F; 2009. http://classic.chem.msu.su/gran/gamess/index.html.